ACS APPLIED MATERIALS & INTERFACES

Research Article

www.acsami.org

Synthesis and Superior Anode Performances of TiO_2–Carbon–rGO Composites in Lithium-Ion Batteries

Yameng Ren,[†] Juan Zhang,[†] Yanyan Liu,[†] Hongbian Li,[‡] Huijuan Wei,[†] Baojun Li,*[,†] and Xiangyu Wang*[,†]

[†]Institute of Industrial Catalysis, College of Chemistry and Molecular Engineering, Zhengzhou University, 100 Science Road, Zhengzhou 450001, P R China

[‡]National Center for Nanoscience and Technology, 11 Beiyitiao Street, Zhongguancun, Beijing 100190, P R China

Supporting Information

ABSTRACT: In this article, TiO_2–Carbon–rGO (GCT) three-component composite material has been constructed by anchoring TiO_2 nanoparticles (NPs) encapsulated in carbon shells onto reduced graphene oxide (rGO) sheets. The structure of GCT was characterized by X-ray diffraction (XRD), Fourier transform infrared (FTIR) spectroscopy, Raman spectroscopy, X-ray photoelectron spectroscopy (XPS), N_2 adsorption–desorption isotherms, and transmission electron microscopy (TEM). This material shows a superior retention as the anode materials in lithium ion battery with a specific discharge capacity of 188 mA h g^{-1} in the initial cycle and 158 mA h g^{-1} after 100 cycles.

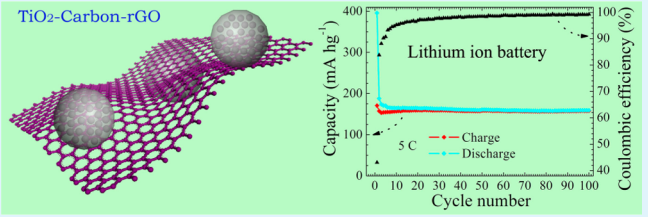

KEYWORDS: *reduced graphene oxide, TiO_2 nanoparticles, core–shell structure, composite materials, lithium ion battery*

1. INTRODUCTION

Since its discovery in 2004, graphene has attracted great research interesting from various fields.[1−3] Graphene sheets are composed of a monolayer sp^2-hybridized carbon atoms. Graphene is endowed with many unique physical and chemical properties, such as very high surface area, superior mechanic rigidity, and electronic transmission.[4−6] The sp^2 hybridized carbon atoms in graphene make it possible to be oxidized and functionalized with many groups, which is usually named graphene oxide (GO). The high surface area and plenty surface functional groups facilitate it to construct novel functional materials.[7−10] The modifications of graphene or reduced GO (rGO) sheets with inorganic nanoparticles (NPs) have been becoming a main strategy to construct graphene-based composite materials. These composite materials have been applied in many various fields, such as in the catalytic oxygen reduction, photocatalytic hydrogen evolution and degradation of organic pollutants, adsorption filtration of dyes, lithium ion batteries (LIBs), supercapacitors and magnetic materials.[11−26] These composite materials exhibit improved performances over pure graphene or rGO. Some drawbacks still remain because the simple components often cannot satisfy the requirements of practical devices.[27,28] One solution is to construct multicomponent composite materials on graphene or rGO sheets.[29−31] It should be expected that the three-dimensional complex structures with multicomponents will generate more novel properties. The constructions of core–shell structures on graphene or rGO sheets have been the successful cases of this strategy.[32−34] The TiO_2 nanostructures have been considered as a promising material for anode of LIBs because of the high capacity and high current rate tolerance.[35,36] However, problems still remained in practical application, for example, the poor conductivity of TiO_2 nanosructures makes an obstacle of current in LIBs, another problem is TiO_2 nanosructures collapsed after being used and this decreases the performance seriously in the cycle test. If graphene or rGO sheets are used to improve the electron conductivity and structure stability of anode materials of TiO_2, the core–shell structures composed of TiO_2 NPs and carbon shells may be an excellent example for the multicomponent composite materials strategy.

In this article, a facile strategy for constructing multicomponent composite materials was demonstrated by anchoring the TiO_2 NPs encapsulated in carbon shells onto rGO sheets. The as-prepared TiO_2–Carbon–rGO (GCT) three component composite materials exhibit improved capacity retention behaviors as an anode material in LIBs.

2. EXPERIMENTAL SECTION

2.1. Materials Synthesis. Graphene oxide (GO) was prepared from natural graphite according to modified Hummers method.[37,38] An aqueous solution (400 mL) of GO (50 mg), Polyethylene glycol (PEG MW10000, 1500 mg), and glucose (1500 mg) was ultrasonicated for 2 h. An ethanol solution (50 mL) of tetra *n*-butyl titanate (8500 mg) were added to the aqueous suspension under stirring and then the mixture was stirred for another 2 h. The mixture was

Received: June 22, 2012
Accepted: August 17, 2012
Published: August 17, 2012

transferred into an autoclave (500 mL) and heated to 160 °C for 24 h. After cooled to room temperature naturally, the resulted solid was washed with water and dried at 140 °C in air. After being heated to 500 °C with a heating rate of 10 °C/min and kept for 2 h in N_2 flow, GCT was obtained.

2.2. Materials Characterization. The phase structure of as−prepared product was characterized with X−ray diffraction (XRD, Bruker D8 advance with Cu Kα λ = 1.5418 Å). Raman spectrum was recorded on a Renishaw RM−1000 with excitation from the 514 nm line of an Ar−ion laser with a power of about 5 mW. Fourier transform infrared (FTIR) spectra measurements were carried out on a NICOLET 380 Fourier transform infrared spectrophotometer. X-ray photoelectron spectrum (XPS) were recorded on a PHI quantera SXM spectrometer with an Al Kα = 280.00 eV excitation source, where binding energies were calibrated by referencing the C1s peak (284.8 eV) to reduce the sample charge effect. The morphology of as−prepared product was studied by using transmission electron microscope (TEM, FEI tecnai G2 electron microscope, operating at 200 kV). N_2 adsorption−desorption isotherm was tested on TriStar II 3020 (Micromeritics Instrument Corporation, USA).

2.3. Electrochemical Measurement. LIBs performance was determined using CR 2032 type coin cells assembled in an argon−filled glovebox (MBRAUN). The working electrodes prepared by mixing the GCT and Carboxymethyl cellulose sodium (CMC, 3 wt %) at a weight ratio of 90:10 were pasted on pure Cu foil (15 μm). Celgard 2400 was used as a separator. Li foil was used as the counter electrode. The electrolyte consisted of a solution of $LiPF_6$ (1 M) containing vinylene carbonate (2 wt %) in ethylene carbonate/dimethyl carbonate/diethyl carbonate (1:1:1, volume ratio). A galvanostatic cycling test of the assembled cells was carried out on a BS-9300K system in the voltage range of 0.001−3.0 V (vs Li^+/Li) at current density of 0.2 (200 mA g^{-1}), 0.5, 1.0, 2.0, 5.0, and 10.0C, respectively. The weight of GCT in the working electrode was used to estimate the specific discharge capacity of the battery, which was expressed in mA h g^{-1} of GCT.

3. RESULTS AND DISCUSSION

An aqueous solution of GO, polyethylene glycol (PEG MW10000), and glucose was ultrasonicated for 2 h (see Scheme 1). An ethanol solution of tetra *n*-butyl titanate was added to the aqueous suspension under stirring and then the mixture was stirred for further 2 h. The mixture was then transferred into an autoclave, heated to 160 °C, and kept there for 24 h. After being cooled to room temperature naturally, the resulting solid was washed with water and dried at 140 °C. According to similar systems in the literature, the appropriate calcination temperature of 500 °C was selected to obtain carbonization of glucose and formation of anatase phase TiO_2.[31,32,39]

Scheme 1. Synthesis Route for Three-Component Composite GCT

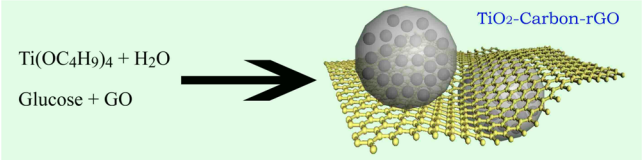

The microstructure of GCT was observed by TEM images (Figure 1). The morphology of composite materials is almost consistent with the rGO sheets in the range of micrometer range. The rGO sheets can be observed clearly in GCT. It also can be observed that the sizes of TiO_2 NPs on rGO are in the range of 10−15 nm. The TiO_2 NPs are anchored onto the rGO sheets, whereas no separate NPs can be observed (Figure 1a).

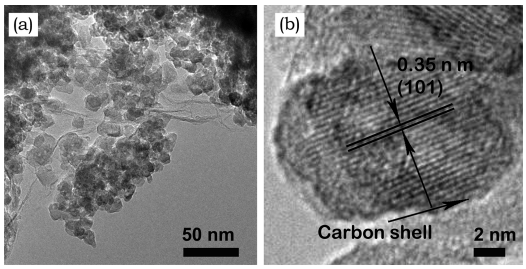

Figure 1. (a) TEM, and (b) high-resolution TEM images of GCT.

The clearly visible set of lattice fringes with a period ~0.35 nm is the characteristic of (101) lattice planes of anatase phase TiO_2 (Figure 1b).[40]

In XRD patterns (Figure 2a), the peaks at 25.3, 37.9, 48.1, 54.1, 55.1, 62.9, 68.9, 70.3, and 75.3° indicate that the TiO_2 NPs in GCT is anatase phase.[41,42] Calculated from the (101) peak in XRD pattern, the crystal size of TiO_2 NPs is 11 nm, which is in agreement with that in TEM images (Figure 1, and Table S2 in the Supporting Information). The unobservable peak at 11.3° show that the reduction of GO to rGO are almost completed. Raman spectra also provide further evidence for the existence of rGO and TiO_2 in GCT (Figure 2b). The G band (1588 cm^{-1}) corresponding to sp^2 hybridized carbon and the D band (1350 cm^{-1}) originating from disordered carbon are observed for rGO.[43] The Raman bands located at 157 cm^{-1} (E_g), 395 cm^{-1} (B_{1g}), 514 cm^{-1} (A_{1g}), and 632 cm^{-1} (E_g) are attributed to the anatase phase TiO_2.[39,42,44] The coexistence of rGO and TiO_2 also were evidenced by FTIR spectra (Figure 2c). The absence of clear peak at 1732 cm^{-1} for carboxyl in GCT indicates the reduction of GO to rGO.[16,18] The band at 400−950 cm^{-1} should be attributed to the Ti−O−Ti stretching vibration modes in TiO_2 NPs.[31,44] In the XPS spectra, the peak at 284.8 eV is the main characteristic of C1s in rGO and carbon shell (Figure 2d).[31,32] The weak peaks at 285.4 and 288.8 eV demonstrate that the epoxide, hydroxyl, and carboxyl groups have been effectively reduced (inset in Figure 2d).[16,18,31,32]

The information of specific surface area and pore structure were obtained from the N_2 adsorption−desorption isotherms of GCT measured at 77 K (Figure 3). The isotherm belongs clearly to type IV. The hysteresis loops indicate that GCT possesses typical mesoporous structures (Figure 3a). From the adsorption branch of isotherm curves, the specific surface area of 167.2 m^2 g^{-1} are calculated for GCT through a multi−point Brunauer−Emmett−Teller (BET) method. From the desorption branch of isotherm curves, the pore width distributions of GCT calculated with Barrett−Joyner−Halenda (BJH) model are concentrated in the range of typical mesoporous structure (Figure 3b). The most probable pore width of 3.8 and 32.5 nm and average pore width of 7.5 nm are calculated for GCT using BJH model. The total pore volumes with pore width from 1.7 to 300 nm are 0.26 cm^3 g^{-1} for GCT. The high specific surface area and typical mesoporous structure of GCT will be useful for the facile diffusion of Li^+ ions in electrodes.[31,32,39] Somewhat improved electrochemical performances of GCT as anode material in LIBs should be expected.[41−43]

A standard method based on GCT-Li half cell was used to evaluate the electrochemical behavior. The theoretical capacity (C) of the hypothetical mixture of GCT is calculated shown as follows

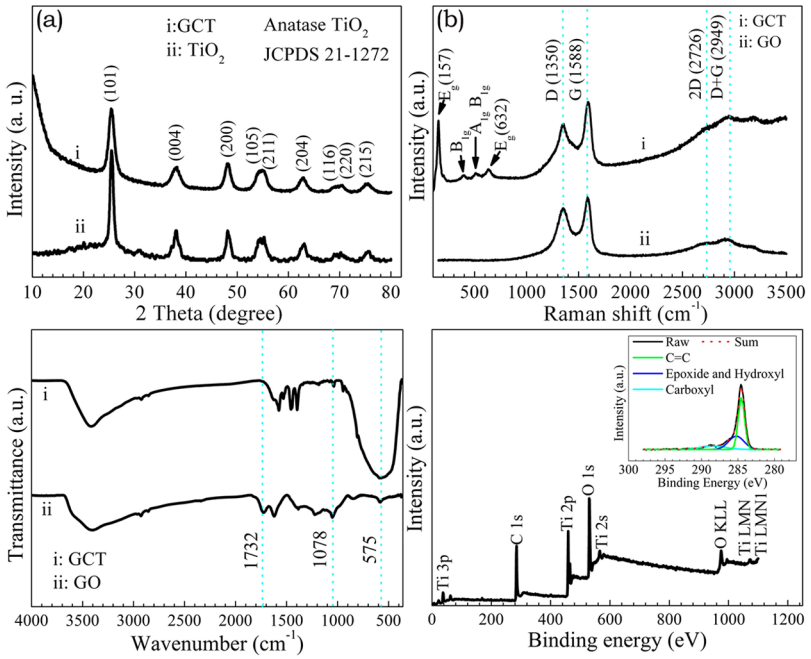

Figure 2. (a) XRD patterns of GCT and TiO_2, respectively, (b) Raman spectra of GCT and GO with excitation laser wavelength of 514 nm, (c) FTIR spectra of GCT and GO, and (d) XPS spectrum of GCT. The inset in d is the fine spectrum of C1s.

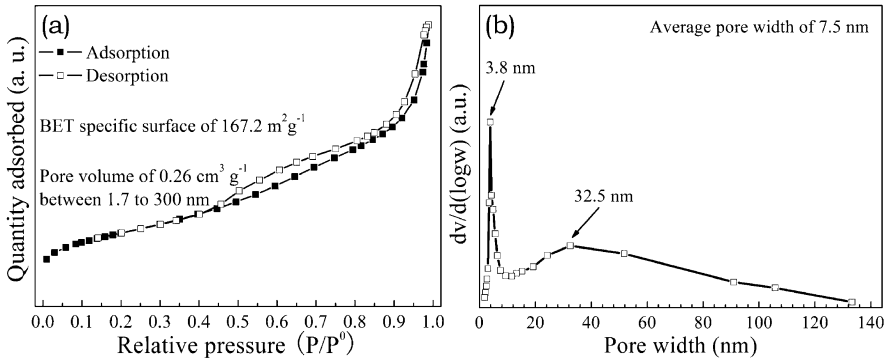

Figure 3. (a) N_2 adsorption–desorption isotherms at 77 K, and (b) pore width distribution of GCT.

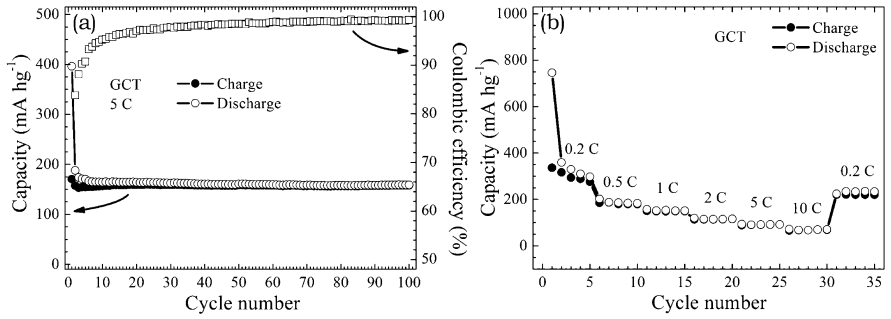

Figure 4. (a) Cycle performance of electrode fabricated with GCT at current rate of 5*C* (1*C* = 200 mA g^{-1}, corresponding to the full discharge in 1 h, a rate of *nC* corresponds to the full discharge in 1/*n* h), and (b) the charge–discharge performances of GCT at various current rates (0.2–10*C*). The weight of GCT in the working electrode was used to estimate the specific discharge capacity of the battery.

$$C_{theoretical} = C_{TiO2}(\text{mass percentage of } TiO_2) + C_{Graphite}(\text{mass percentage of graphite})$$
$$= 168 \cdot 85\% + 372 \cdot 15\%$$
$$= 199 \text{ mA h g}^{-1}$$

$$Li^+ + e^- \rightarrow SEI(Li) \quad (1)$$

$$GCT + xLi^+ + xe^- \leftrightarrow Li_xTiO_2 - carbon - rGO \quad (2)$$

$$xLi \leftrightarrow xLi^+ + xe^- \quad (3)$$

At a current rate of 5*C*, the initial capacity is obtained as 396 mA h g^{-1} for GCT, which is higher than the reversible capacity

from the second cycle (195 mA h g^{-1}) and the theoretical capacity of the hypothetical mixture of GCT (Figure 4a). The second and third discharge processes also exhibit reversible discharging behavior, with a decrease in the discharge capacity. The discharge capacities of the electrode in second, third, fourth and fifth cycles are 188, 174, 171, and 170 mA h g^{-1}, respectively (Figure 4a). The reversible capacity after 100 cycles is observed to be 158 mA h g^{-1}, which is 93% of the discharge capacities in fifth cycle. At various current density (current rates of 0.2−10C), some high discharge capacity (≥95.5 mA h g^{-1}) are obtained for GCT (Figure 4b). After charging-discharging at higher current rates of 0.5, 1, 2, 5, and 10C, the high capacities can be remained for GCT at normal current rate of 0.2*C* (Figure 4b). These reversible capacities showed clearly that superior rechargeable stability can be obtained with GCT as the anode materials. It is noteworthy that the cyclic performances of GCT are higher than those of TiO_2−carbon composite prepared without rGO (see Figure S4 in the Supporting Information).[45] These specific capacities and rechargeable stability are comparable to the hierarchical spheres from large ultrathin anatase TiO_2 nanosheets with nearly 100% exposed (001) facets.[46] Further study is needed to understand the detailed electrochemical behavior GCT in the electrode.[47]

4. CONCLUSIONS

In conclusion, a simple and scalable approach for the preparation of three-component composite materials GCT was developed. Because of the coexistence of carbon shells and rGO sheets, GCT possesses superior structure stability with high specific surface area and excellent electronic conductivity. As an anode material for LIBs, the cycle performance of GCT has been determined for 100 cycles with high capacity and excellent cycle stability. GCT exhibited a specific discharge capacity of 188 mA h g^{-1} in the initial cycle and 158 mA h g^{-1} after 100 cycles. From these results, it should be concluded that GCT are very promising materials used as the anode of LIBs. The concept of three-dimensional complex structures and the preparation approach will find their application in the field of storage energy devices.

■ ASSOCIATED CONTENT

Supporting Information

Experimental section and additional figures and tables (PDF). This material is available free of charge via the Internet at http://pubs.acs.org.

■ AUTHOR INFORMATION

Corresponding Author

*E-mail: lbjfcl@zzu.edu.cn (B.L.); xiangyuwang@zzu.edu.cn (X.W.).

Notes

The authors declare no competing financial interest.

■ ACKNOWLEDGMENTS

Financial support from the China Postdoctoral Science Foundation (2012M511121) and the Innovation Fund for Elitists of Henan Province, China (0221001200), is greatly acknowledged.

■ REFERENCES

(1) Novoselov, K. S.; Geim, A. K.; Morozov, S. V.; Jiang, D.; Zhang, Y.; Dubonos, S. V.; Grigorieva, I. V.; Firsov, A. A. *Science* **2004**, *306*, 666−669.
(2) Rao, C. N. R.; Sood, A. K.; Subrahmanyam, K. S.; Govindaraj, A. *Angew. Chem., Int. Ed.* **2009**, *48*, 7752−7777.
(3) Allen, M. J.; Tung, V. C.; Kaner, R. B. *Chem. Rev.* **2010**, *110*, 132−145.
(4) Robinson, J. T.; Tabakman, S. M.; Liang, Y. Y.; Wang, H. L.; Casalongue, H. S.; Vinh, D.; Dai, H. J. *J. Am. Chem. Soc.* **2011**, *133*, 6825−6831.
(5) Guo, C. X.; Yang, H. B.; Sheng, Z. M.; Lu, S. Z.; Song, Q. L.; Li, C. M. *Angew. Chem., Int. Ed.* **2010**, *49*, 3014−3017.
(6) Yao, F.; Gunes, F.; Ta, H. Q.; Lee, S. M.; Chae, S. J.; Sheem, K. Y.; Cojocaru, C. S.; Xie, S. S.; Lee, Y. H. *J. Am. Chem. Soc.* **2012**, *134*, 8646−8654.
(7) Gulbakan, B.; Yasun, E.; Shukoor, M. I.; Zhu, Z.; You, M. X.; Tan, X. H.; Sanchez, H.; Powell, D. H.; Dai, H. J.; Tan, W. H. *J. Am. Chem. Soc.* **2010**, *132*, 17408−17410.
(8) Wang, H. L.; Yang, Y.; Liang, Y. Y.; Robinson, J. T.; Li, Y. G.; Jackson, A.; Cui, Y.; Dai, H. J. *Nano Lett.* **2011**, *11*, 2644−2647.
(9) Wang, H. L.; Yang, Y.; Liang, Y. Y.; Cui, L. F.; Casalongue, H. S.; Li, Y. G.; Hong, G. S.; Cui, Y.; Dai, H. J. *Angew. Chem., Int. Ed.* **2011**, *50*, 7364−7368.
(10) Wang, H. L.; Liang, Y. Y.; Li, Y. G.; Dai, H. J. *Angew. Chem., Int. Ed.* **2011**, *50*, 10969−10972.
(11) Liang, Y. Y.; Li, Y. G.; Wang, H. L.; Zhou, J. G.; Wang, J.; Regier, T.; Dai, H. J. *Nat. Mater.* **2011**, *10*, 780−786.
(12) Liang, Y. Y.; Wang, H. L.; Zhou, J. G.; Li, Y. G.; Wang, J.; Regier, T.; Dai, H. J. *J. Am. Chem. Soc.* **2012**, *134*, 3517−3523.
(13) Li, Y. G.; Wang, H. L.; Xie, L. M.; Liang, Y. Y.; Hong, G. S.; Dai, H. J. *J. Am. Chem. Soc.* **2011**, *133*, 7296−7299.
(14) Lightcap, I. V.; Kamat, P. V. *J. Am. Chem. Soc.* **2012**, *134*, 7109−7116.
(15) Liang, Y. Y.; Wang, H. L.; Casalongue, H. S.; Chen, Z.; Dai, H. J. *Nano Res.* **2010**, *3*, 701−705.
(16) Li, B. J.; Cao, H. Q. *J. Mater. Chem.* **2011**, *21*, 3346−3349.
(17) Zhou, G. M.; Wang, D. W.; Li, F.; Zhang, L. L.; Li, N.; Wu, Z. S.; Wen, L.; Lu, G. Q.; Cheng, H. M. *Chem. Mater.* **2010**, *22*, 5306−5313.
(18) Li, B. J.; Cao, H. Q.; Shao, J.; Zheng, H.; Qu, M. Z. *Chem. Commun.* **2011**, *47*, 3159−3161.
(19) Wang, H. L.; Cui, L. F.; Yang, Y. A.; Casalongue, H. S.; Robinson, J. T.; Liang, Y. Y.; Cui, Y.; Dai, H. J. *J. Am. Chem. Soc.* **2010**, *132*, 13978−13980.
(20) Bhardwaj, T.; Antic, A.; Pavan, B.; Barbone, V.; Fanlman, B. D. *J. Am. Chem. Soc.* **2010**, *132*, 12556−12558.
(21) Yin, Y. J.; Hu, Y. J.; Wu, P.; Zhang, H.; Cai, C. X. *Chem. Commun.* **2012**, *48*, 2137−2139.
(22) Zhou, X. S.; Yin, Y. X.; Wan, L. J.; Guo, Y. G. *Chem. Commun.* **2012**, *48*, 2189−2200.
(23) Wang, H. L.; Casalongue, H. S.; Liang, Y. Y.; Dai, H. J. *J. Am. Chem. Soc.* **2010**, *132*, 7274−7477.
(24) Wang, H. L.; Liang, Y. Y.; Mirfakhrai, T.; Chen, Z.; Casalongue, H. S.; Dai, D. J. *Nano Research* **2011**, *4*, 729−736.
(25) Chen, Z.; Hong, G. S.; Wang, H. L.; Welsher, K.; Tabakman, S. M.; Sherlock, S. P.; Robinson, J. T.; Liang, Y. Y.; Dai, H. J. *ACS Nano* **2012**, *6*, 1094−1101.
(26) Zhu, G. X.; Liu, Y. J.; Xu, Z.; Jiang, T. A.; Zhang, C.; Li, X.; Qi, G. *ChemPhysChem* **2012**, *11*, 2432−2437.
(27) Chen, X. C.; Wei, W.; Lv, W.; Su, F. Y.; He, Y. B.; Li, B. H.; Kang, F. Y.; Yang, Q. H. *Chem. Commun.* **2012**, *47*, 5904−5906.
(28) Luo, B.; Wang, B.; Liang, M. H.; Ning, J.; Li, X. L.; Zhi, L. J. *Adv. Mater.* **2012**, *24*, 1405−1409.
(29) Zhou, X. S.; Yin, Y. X.; Cao, A. M.; Wan, L. J.; Guo, Y. G. *ACS Appl. Mater. Interfaces* **2012**, *4*, 2824−2828.
(30) Su, C.; Bu, X. D.; Xu, L. H.; Liu, J. L.; Zhang, C. *Electrochim. Acta* **2012**, *64*, 190−185.

(31) Li, B. J.; Cao, H. Q.; Shao, J.; Qu, M. Z. *Chem. Commun.* **2011**, *47*, 10374−10376.
(32) Li, B. J.; Cao, H. Q.; Zhang, J. X.; Qu, M. Z.; Lian, F.; Kong, X. H. *J. Mater. Chem.* **2012**, *22*, 2851−2854.
(33) Xue, D. J.; Xin, S.; Yin, Y.; Jiang, K. C.; Yin, Y. X.; Guo, Y. G.; Wan, L. J. *J. Am. Chem. Soc.* **2012**, *134*, 2512−2515.
(34) Zhang, C. F.; Peng, X.; Guo, Z. P.; Cai, C. B.; Chen, Z. X.; Wexler, D.; Li, S.; Liu, H. K. *Carbon* **2012**, *50*, 1897−1903.
(35) Li, N.; Liu, G.; Zhen, C.; Li, F.; Zhang, L. L.; Cheng, H. M. *Adv. Funct. Mater.* **2011**, *21*, 1717−1722.
(36) Ding, S. J.; Chen, J. S.; Luan, D. Y.; Boey, F. Y. C.; Madhavi, S.; Lou, X. W. *Chem. Commun.* **2011**, *47*, 5780−5782.
(37) Hummers, W. S.; Offeman, R. E. *J. Am. Chem. Soc.* **1958**, *80*, 1339−1339.
(38) Li, B. J.; Cao, H. Q.; Shao, J.; Li, G. Q.; Qu, M. Z.; Yin, G. *Inorg. Chem.* **2011**, *50*, 1628−1632.
(39) Cao, H. Q.; Li, B. J.; Zhang, J. X.; Lian, F.; Kong, X. H.; Qu, M. Z. *J. Mater. Chem.* **2012**, *22*, 9759−9766.
(40) Wu, H. B.; Hng, H. J.; Lou, X. W. *Adv. Mater.* **2012**, *24*, 2567−2571.
(41) Wu, H. B.; Lou, X. W.; Hng, H. H. *Chem.−Eur. J.* **2012**, *18*, 2094−2099.
(42) Liu, J. H.; Chen, J. S.; Wei, X. F.; Lou., X. W.; Liu, X. W. *Adv. Mater.* **2011**, *23*, 998−1002.
(43) Ni, Z. H.; Wang, H. M.; Kasim, J.; Fan, H. M.; Yu, T.; Wu, Y. H.; Feng, Y. P.; Shen, Z. X. *Nano Lett.* **2007**, *7*, 2758−2763.
(44) Jiang, B. J.; Tian, C. G.; Zhou, W.; Wang, J. Q.; Xie, Y.; Pan, Q. J.; Ren, Z. Y.; Dong, Y. Z.; Fu, D.; Han, J. L.; Fu, H. G. *Chem.−Eur. J.* **2011**, *17*, 8379−8387.
(45) Cao, F. F.; Wu, X. L.; Xin, S.; Guo, Y. G.; Wan, L. J. *J. Phys. Chem. C* **2010**, *114*, 10308−10313.
(46) Chen, J. S.; Tan, Y. L.; Li, C. M.; Cheah, Y. L.; Luan, D. Y.; Madhavi, S.; Boey, F. Y. C.; Archer, L. A.; Lou, X. W. *J. Am. Chem. Soc.* **2010**, *132*, 6124−6130.
(47) Wang, Y. Q.; Guo, L.; Guo, Y. G.; Li, H.; He, X. Q.; Tsukimoto, S.; Ikuhara, Y.; Wan, L. J. *J. Am. Chem. Soc.* **2012**, *134*, 7874−7879.